

Experimental evidence for a chiral symmetry-breaking mechanism in aspartic acid: Lattice and sub-lattice matching



Omar Teschke*, David Mendez Soares

Laboratorio de Nanoestruturas e Interfaces, Instituto de Física, UNICAMP, 13083-859 Campinas, SP, Brazil

ARTICLE INFO

Article history:

Received 27 January 2017

Received in revised form 7 June 2017

Accepted 9 June 2017

Available online 13 June 2017

Communicated by Gen Sazaki

Keywords:

Aspartic acid

Preferential crystallization mechanism

Chiral symmetry-breaking mechanism

ABSTRACT

A mother crystal formed from a transient molecular structure of (D+L) aspartic acid in solution is reported. Hexagonal structures with a lattice constant of 1.04 nm were crystallized from a solution in which three aspartic acid species coexist: right- and left-handed enantiomorphs, denoted D-aspartic and L-aspartic, respectively, and transitory (D+L) aspartic acid specie. Atomic force microscopy images of the crystalline deposits reveal domains of the transitory (D+L) aspartic acid crystal forming the substrate deposit on silicon wafers, and on top of this hexagonal lattice only L-aspartic acid is observed to conform and crystallize. A preferential crystallization mechanism is then observed for (D+L) aspartic acid crystals that seed only L-aspartic deposits by the geometrical matching of their multiple hexagonal lattice structures with periodicities of 1.04 nm and 0.52 nm, respectively.

© 2017 Elsevier B.V. All rights reserved.

1. Introduction

Geometric preferences favoring one enantiomer over its mirror image are observed in the structures of amino acids, sugars and biopolymers in living organisms. How these chiral asymmetries spontaneously arose in the terrestrial biosphere is a puzzling question. Physical or chemical processes commonly yield a racemic mixture of both D- and L-enantiomers [1,2]. Several mechanisms have been proposed [3–8] to explain the spontaneous appearance of chiral asymmetries from a presumably unbiased prebiotic terrestrial environment, but unified view to explain biohomochirality has not been obtained because of the lack of conclusive experimental demonstrations.

Crystallization is still an important means by which chiral molecules are separated into their two mirror-image isomers (enantiomers) [9]; however, this process remains poorly understood [10]. A result that could clarify some aspects of the crystallization mechanism was reported by Lee and Lin [11]. They experimentally showed using Fourier transformed infrared spectroscopy and powder X-ray diffraction, that the crystalline structure produced by a solution of a racemate aspartic acid (DL-asp) was different from the crystalline structure obtained from an aqueous solution prepared by dissolving equal amounts of D-asp and L-asp, defined as the (D+L)-asp solution. This report was followed

by the work of Wang et al. [12] who used high-resolution solid-state ^{13}C NMR with cross-polarization and magic-angle spinning to study chirality in the crystallization of aspartic acid. Contrary to the report of Lee and Lin [11], they showed that DL-asp crystallizes over most of its temperature range as racemic crystals rather than as a conglomerate of enantiomeric crystals, regardless of whether the solution was prepared by dissolving D-asp and L-asp and mixing the solutions or prepared by dissolving DL-asp. In order to clarify the variance in the above reported results we have investigated the crystallization differences between DL-asp solutions and solutions prepared by mixing solutions of D-asp and L-asp. To observe the possible differences we have used atomic force microscopy (AFM) in an arrangement that results in molecular resolution as shown by our recently reported results that depict a new molecular arrangement of L-asp with a hexagonal structure and a lattice parameter of ~ 0.51 nm [13].

Associated with geometrical preferences favoring one enantiomer over its mirror image there is the mother crystal phenomenon. Recently Viedma [14] has experimentally demonstrated for sodium chlorate (NaClO_3) total chiral symmetry breaking in the absence of specific mother crystal which is achieved through a nonlinear autocatalytic recycling process. Here however we report on the discovery of a new racemic aspartic acid structure which plays the role of the mother crystal formed in the crystallization of aspartic acid. We have also investigated the handedness of this mother crystal and its effect in the aspartic acid chiral symmetry breaking mechanism.

* Corresponding author.

E-mail address: oteschke@ifi.unicamp.br (O. Teschke).

2. Experimental

We prepared three different solutions by dissolving D-, L- and DL-asp in distilled, deionized water (Milli-Q, 18 M Ω /cm), and each component was dissolved to near (\sim 100%) saturation. D-asp, L-asp and DL-asp of high purity were purchased from Sigma Chemical Company, USA. The resulting solutions were constantly stirred to ensure complete dissolution of the solute. Deposits were formed on single-crystal, polished (100) oriented wafers of doped (p-type) silicon and 0.4 Ω cm resistivity (lightly doped), which were cut into rectangles with areas of approximately 1.0 cm². Previous to use the substrates were etched in a bath solution prepared by admixture of equal volumes of aqueous 48% HF (Merck) and 95% ethanol (Merck) and then 100 μ l drops of the resultant solution were dried on silicon wafers.

All experiments were performed in parallel and in independent series that were repeated several times. The drying method used to evaporate water and grow solids was air-drying at 25 $^{\circ}$ C with 60% relative humidity. All dried solids were examined by polarized optical microscopy, AFM and confocal Raman microscopy (CRM). Optical images were recorded using an AxioPlan universal microscope (Carl Zeiss D-7082, Germany) with computer-assisted digital imaging. The Raman spectrum was obtained using a scanning near-field optical microscope (SNOM-CRM200, Witec, Germany). We also used an AFM (model TMX2000, TopoMetrix) with silicon nitride (Si₃N₄) tips (Microlevers, Veeco, model MSCT-AUHW) and spring constants of approximately 0.03 N/m to image surface structure of the crystal deposited on the silicon substrate with molecular resolution. The radius of curvature of the AFM tip was approximately 5 nm. The scan velocity was optimized to obtain the best signal-to-noise ratio, thereby resulting in a value of \geq 100 nm/s for operation in air. The patterns shown correspond to the best signal-to-noise ratio images of the various scanned samples. The AFM was operated in lateral force mode, in which all feedback loops were opened without a scanning velocity limitation by the time constant of the piezoelectric translator and feedback circuits [15].

3. Results and discussion

In our previous work the surface structure of D-asp, L-asp and DL-asp crystals deposited on various substrates was investigated [13]. The crystal structure was characterized by measuring its lattice parameters shown in the AFM images. The spectroscopic data also is demonstrated by the fast Fourier transform (FFT) spectra. The FFT spectrum acquisition of the AFM images uses a different technique than that used by bulk crystal in X-ray crystallography. The spatial periodicity of a crystal along scanned direction is calculated using the measured profiles for each line, the two-dimensional power spectrum was acquired combining line scans and forming the profile in the orthogonal directions. The measured lattice parameters are depicted in Table 1 as revealed in our previ-

ous work [8] and for comparison the X-ray diffraction data for L-asp and D-asp where $a = 0.76$ nm, $b = 0.69$ nm and $c = 0.51$ nm and for DL-asp where $a = 1.75$ nm, $b = 0.74$ nm and $c = 0.91$ nm [17–19,6].

Here we investigated different macroscopic precipitation patterns characterized by its crystal morphology and its Raman spectrum for mixtures of equal amounts of D-asp and L-asp in solutions dried on silicon substrates. The crystals formed from this solution are shown in Fig. 1(i, ii). In Fig. 1 it is possible to observe differences in the deposits structures. The deposit indicated by (a) shows a geometric pattern defined by crystalline planes while in deposit (b) there are no observable crystalline planes. To chemically characterize the differences between the substrate deposit (a) and the top deposit (b), the Raman spectra of these crystals were recorded. Fig. 2(i) shows the Raman spectrum of the substrate deposit (spectrum a) and the top deposit (spectrum b). The spectra of the substrate and the top deposits show different peak distributions as

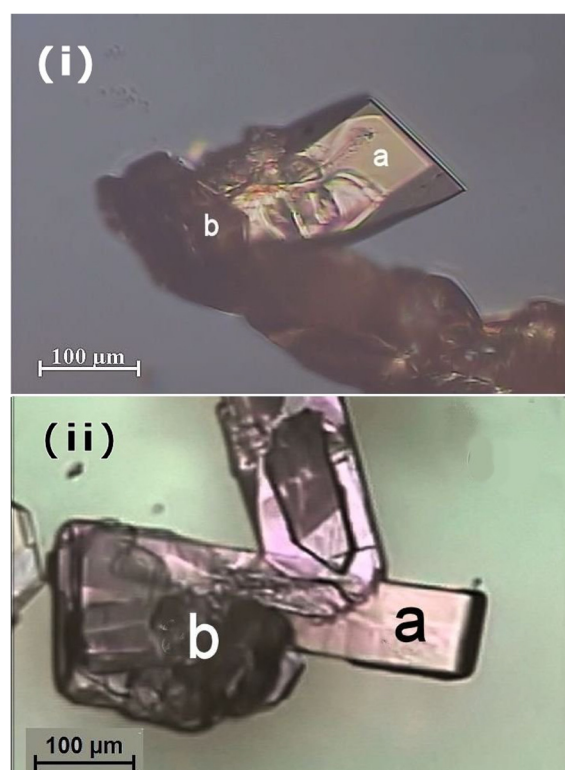


Fig. 1. Optical images of aspartic acid deposits on silicon substrates. Two macroscopic precipitation patterns can be observed by differences in morphology, a substrate bottom layer (indicated by a) and a top layer (indicated by b). The silicon substrate is a flat polished surface; the substrate deposit forms a solid structure with sharp edges and almost flat surfaces forming geometric patterns defined by crystalline planes. The top layer indicated by (b) shows a surface with irregular pattern deposits and no crystalline planes.

Table 1

Lattice parameter data (a,b,c) of standard L-asp, D-asp and DL-asp films measured by AFM on the top line and the X-ray diffraction data on the bottom line. The right column list the transient compound L-asp crystalline structure measured in our previous work, and the new (D+L)-asp with a hexagonal lattice structure and lattice parameters $a = b = 1.02$ nm.

Standard compounds	Transient compounds in solution						
	Measured Crystal Structure (top) X-ray Diffraction [17–19,6] (bottom)	L-asp	D-asp	DL-asp	Hexagonal crystal structure (nm)	L-asp	(D+L)-asp
a (nm)		0.76	0.76	1.75		0.52	1.04
		0.7617	0.7617	1.7581			
b (nm)		0.69	0.69	0.74			
		0.6982	0.6982	0.74369			
c (nm)		0.51	0.51	0.91			
		0.5143	0.5143	0.91807			

Download English Version:

<https://daneshyari.com/en/article/5489326>

Download Persian Version:

<https://daneshyari.com/article/5489326>

[Daneshyari.com](https://daneshyari.com)